Journal of The Electrochemical Society, **155** (3) K31-K37 (2008)
0013-4651/2008/155(3)/K31/7/$23.00 © The Electrochemical Society

Passivity of a Nanostructured Directionally Solidified NiAl–Re Alloy as Substrate for Electrodeposition of Gold

Belen Bello Rodriguez and Achim Walter Hassel[*,z]

Max-Planck-Institut für Eisenforschung GmbH, 40237 Düsseldorf, Germany

Directionally solidified NiAl–Re eutectic alloys can be employed as substrates for the formation of gold nano- and microelectrodes by electrodeposition of this metal in the nanofibers present in the eutectic structure. An initial polarization of the eutectic is required in order to passivate the NiAl matrix and thus confine the electrodeposition process to the fibrous phase. The effect of the applied polarization potential as well as the duration of the treatment were investigated and related to the nucleation process during electrodeposition. It was found that polarization at low anodic potentials (0 V) resulted in a poor passivation of the NiAl matrix, thus yielding gold deposits randomly distributed over the whole surface of the sample. Polarization at high anodic potentials (0.7 V) is essential to ensure that the matrix is fully passive, with the fibrous phase remaining as the only electrochemically active area. The impedance measurements carried out on the samples after polarization at 0.7 V for longer time intervals showed a decrease in resistance after a sufficiently long passivation, attributed to the formation of a porous oxide film and partial corrosion of the sample through the pores created during the process. The polarization time must therefore be confined to 15–20 min to avoid undesirable corrosion. Under these conditions, electrodeposition of gold takes place along the pores left by the dissolution of the fibrous phase and originates arrays of aligned gold microspheres.
 [DOI: 10.1149/1.2823741]

Manuscript submitted June 19, 2007; revised manuscript received October 29, 2007. Available electronically January 2, 2008.

Template electrodeposition is a widely employed technique for the production of well-patterned metallic structures because of the quality of the obtained deposits as well as the relatively simple equipment required and the low cost of the procedure.[1,2] The method can be applied at industrial levels and often can be used in a wider range of geometries than other conventional deposition processes.[3] Template electrodeposition is normally carried out on a variety of substrates, including polycarbonate membranes, nanochannel alumina, or anodized aluminum oxide.[4] The latter possesses a series of properties that make it an attractive template for the formation of nanowires by electrodeposition; it has good mechanical strength and thermal stability and yields the formation of highly ordered arrays of nanostructures.[5] Thus, aluminum oxide has been previously employed as a template for electrodeposition of various metals, such as palladium,[4] nickel,[6] cadmium sulfide,[7] or even Ni–Fe–Co alloys.[8] The use of aluminum oxide as a template usually requires the anodization of aluminum under aggressive conditions,[9] followed by the partial digestion of the oxide layer to open up the blocked ends of the channels present in the templates structure. Alternatively, recent investigations have focused on the formation of aluminum oxide templates by a procedure in which the chemical formation steps are more user-friendly, which would obviate the preliminary electropolishing at high overpotentials and strong acidic conditions as well as the subsequent etching.[10] The use of eutectic alloys which present aluminum as a major component in their composition appears as an attractive alternative. Directionally solidified (ds) NiAl–Re (ds-NiAl–Re) eutectics have therefore been investigated for their suitability as templates for the electrodeposition of metallic nanowires. A mild electrochemical oxidation enables the simultaneous passivation of the aluminum and nickel matrix alongside the dissolution of the fibrous phase composed of Re.[10] The subsequent electrodeposition process enabled the formation of arrays of gold microstructures deposited onto the fibers present in the eutectic. However, the method described presented the drawback of creating gold deposits with a size much larger than the desired scale to obtain nanoelectrodes. The deposits often grew larger than the pores and protruded onto the surface, thus resulting in arrays of microspheres whose combined electrochemical behavior was comparable to conventional macroelectrodes due to overlapping of the diffusion layer of each gold microdeposit. The formation of arrays of gold nanoelectrodes from the studied ds-NiAl–Re eutectic alloys implies the exclusive deposition of the metal along the pore length. To control the pore filling, an exhaustive analysis of electrochemical data was carried out in order to determine the kinetics of the different processes involved (i.e., NiAl passivation, oxidation of Re, and nucleation and growth of gold deposits). In this paper the effect of polarization conditions on the passivation of the eutectics, as well as on the fibers dissolution, is described.

Experimental

NiAl–Re eutectics were directionally solidified as described previously.[11] As a starting material, nickel (99.97 wt %), electrolytic aluminum (99.9999 wt %), and rhenium pellets (99.9 wt %) were used for the alloy preparation Directional solidification was conducted at a temperature of 1690 ± 10°C, a thermal gradient of approximately 40 K cm^{-1}, and a growth rate of 8.3 μm s^{-1}. A diameter of 400 nm was found for the rhenium wires, and the mean interfiber spacing was 3 μm. The fiber orientation was (100), referring to the rod axis of the directionally solidified sample.

Electrochemical passivation of the NiAl and ds-NiAl–Re specimens was carried out by polarization of the samples (area = 1 cm^2) in 1 M acetate buffer (pH 6.0). A conventional three-compartment cell (approx. volume 50 mL) with working, reference, and auxiliary electrodes was employed in all experiments. The samples were mechanically mirrorlike ground and polished and grinded prior to measurements. A commercial Ag/AgCl electrode was used as the reference electrode (Metrohm, Filderstadt, Germany). A smooth Au foil electrode was employed as the counter electrode (apparent surface area = 2 cm^2). For the polarization of Re, a metal wire (diameter = 0.5 mm, purity 99.9%, Johnson Matthey) was submerged in 1 M acetate buffer, and the experiments were performed as previously explained for the NiAl and ds-NiAl–Re samples. A PST050 potentiostat (Radiometer Analytical, Lyon, France) was used in all electrochemical measurements. Measurements were performed at room temperature in quiescent solutions. All potentials are given vs the standard hydrogen electrode (SHE).

The electrodeposition of gold was carried from a commercial bath containing 12 g L^{-1} of gold sulfite in neutral pH (Metakem, Usingen, Germany). The plating was carried out by application of rectangular reverse pulses.[12] The potential was switched from −0.7 to 0.1 V (against anode) at a ratio of 1:10. All experiments were performed at room temperature in nondeaerated solutions.

Electrochemical impedance spectra were recorded with a setup including a Princeton Applied Research potentiostat/galvanostat

* Electrochemical Society Active Member.
[z] E-mail: hassel@elchem.de

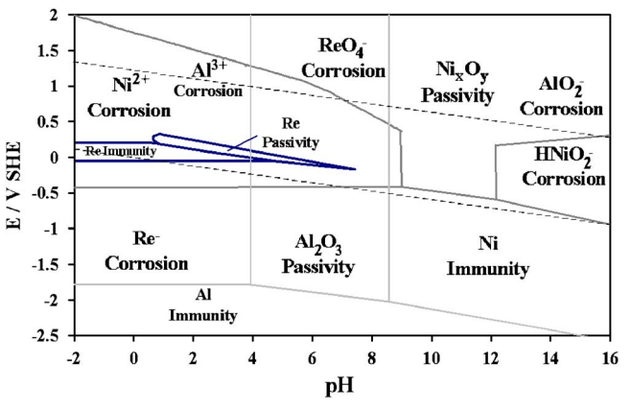

Figure 1. (Color online) Combined *E*–pH diagram for NiAl–Re.

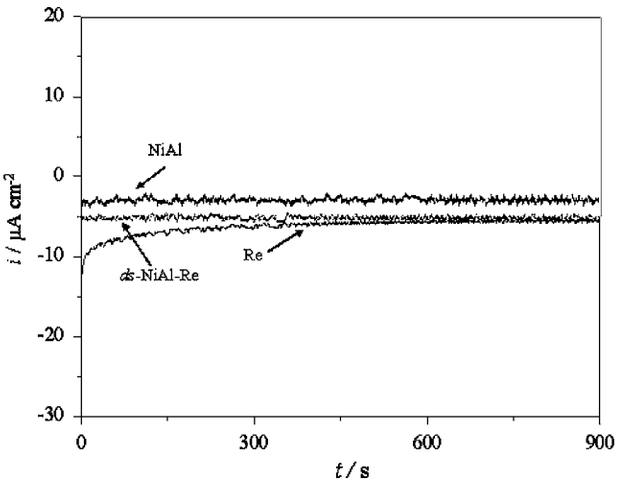

Figure 2. Current transients recorded for the polarization of NiAl, Re, and ds-NiAl–Re in neutral acetate buffer (pH 6.0) at 0 V (vs SHE).

model 283 and a Solartron SI 1260 impedance gain/phase analyzer. The perturbation signal used in the impedance measurements was 1 mV (root mean square).

Scanning electron microscopy pictures were obtained on a Leo 1550 VP apparatus (Leo Elektronenmikroskopie GmbH, Oberkochen, Germany) fitted with a INCA energy-dispersive system (Oxford Instruments, Oxford, U.K.). All materials used were of analytical grade and purchased by Merck (Darmstadt, Germany).

Results and Discussion

Passivation of ds-NiAl–Re at 0 V.— The electrodeposition of gold on the rhenium fibers present in a ds-NiAl–Re eutectic alloy is feasible providing that the matrix is previously passivated to inhibit any electrodeposition that may occur on its surface. This passivation must be done without formation of rhenium oxides on the surface of the fibers, which would otherwise hinder their plating with gold. For the fibers to remain electrochemically active and the matrix to be passive, an appropriate pretreatment must be carried out at an optimal potential. A careful examination of the *E*–pH diagram for each of the elements of the system (Ni, Al, and Re) enables one to establish the optimal experimental conditions for the simultaneous formation of passive Al_2O_3 and NiO oxides, with Re remaining in the metallic phase (Fig. 1, adapted from Ref. 13). Al_2O_3 is formed over a wide range of *E* and pH, and therefore passivation of the matrix by formation of this oxide should not present a problem. Metallic rhenium has a small immunity range, and it easily forms various oxides or soluble anionic species such as perrhenate ions. Re remains in the metallic state at acidic pH values (0–4) and potential values close to 0 V. However, under those potential and pH values, both aluminum and nickel seem to form ionic species and dissolve into the solution. The formation of aluminum and nickel oxides takes place at neutral or basic pH values. This basic pH favors the oxidation of rhenium to perrhenate, which is soluble in the solution, and is the base for the formation of nanopores in the studied eutectics. For a better understanding of NiAl passivation, an initial polarization was done at low anodic potentials to induce the formation of Al_2O_3 oxide on the samples surface, while allowing Re to remain in the metal state. In order for this to occur, the experimental conditions must be compromised, and thus a polarization of the samples at 0 V and pH 6.0 was carried out prior to electrodeposition. As one of the major components of the matrix, the oxidation of aluminum to Al_2O_3 under those experimental conditions is expected to passivate the NiAl matrix enough to hinder any electrochemical reactivity. At those potential and pH values, nickel may form hydroxide species that would further passivate the surface. However, rhenium is also expected to form an oxide, which may hinder the gold electrodeposition. The current transients recorded for the polarization of a ds-NiAl–Re sample at 0 V showed a signal with a value fluctuating at $\sim(-5)$ μA cm^{-2} range (Fig. 2). The negligible current observed at this potential may be explained by a possible hindrance of the matrix oxidation by the presence of an Al_2O_3 layer on the surface of the sample, formed by the sample contact with air. It has been reported that the exposure of wet Ni samples to air leads to the formation of a thin NiO oxide layer,[14] and thus this process would also have affected the conductivity of our specimen. Further formation of oxides on the sample during the polarization period results in a more uniform coverage of the surface, thus decreasing even more the recorded current. Overall, the presence of a passive layer on the matrix, along with slight passivation of the fibers, results in a negligible current when the samples are polarized at 0 V.

The contributions of each of the involved elements on the process were examined by comparing the obtained current transients for the ds-NiAl–Re eutectic at 0 V, recorded for NiAl and Re independently under the same experimental conditions. For NiAl polarization, the recorded current presented a similar value to that previously obtained for the analysis of ds-NiAl–Re (Fig. 2). As suggested for the analysis of ds-NiAl–Re specimens, the low current value observed may be attributed to the presence of passive oxides on the matrix surface. For analysis of Re, the current density increased from an initial value of $\sim(-14)$ μA cm^{-2} to a value of -8 μA cm^{-2} after approximately 75 s and remained constant for longer polarization times (Fig. 2). The initial current increase may be attributed to oxidation of the metal and formation of an oxide layer, the later plateau due to the growth of the ReO_2 or Re_2O_3 oxide.[15] The exact nature of the formed oxide is a matter of controversy, and its elucidation is beyond the scope of this paper.

After polarization of each of the studied samples (NiAl, ds-NiAl–Re, and Re), impedance measurements were carried out and the *Z* and θ values were plotted against the examined frequency range (Fig. 3). In all three cases, the impedance values recorded were higher at lower frequencies, and the total impedance was larger for the ds-NiAl–Re system than for NiAl. This could be attributed to a more efficient passivation of the sample surface due to the presence of rhenium oxides. For both ds-NiAl–Re and NiAl, the impedance diagrams can be described by a simple electrical circuit comprising of the resistance of the electrolyte ($\sim 10\ \Omega$) in series with the capacitor *C* and resistor *R* of the sample's double layer and/or the native oxide layer present in the sample. The values of *C* and *R* were obtained by fitting the experimental data into the equivalent circuit described. The thickness of the oxide layer can therefore be calculated according to

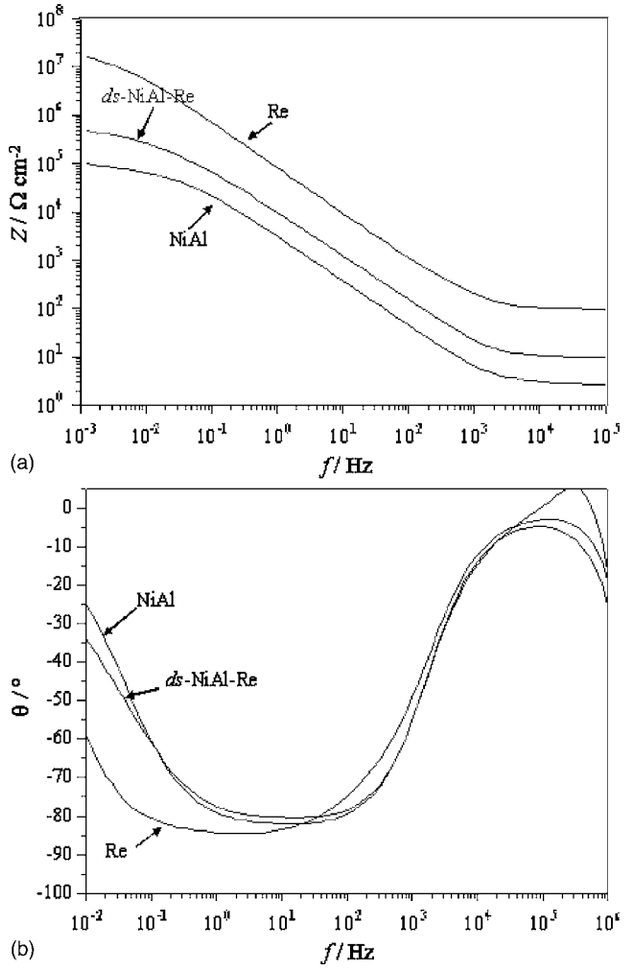

Figure 3. EIS spectra obtained for NiAl, Re, and NiAl–Re after polarization of the samples in acetate buffer for passivation of the matrix at 0 V.

$$C = \frac{\varepsilon \varepsilon_o}{d} \quad [1]$$

where ε_o is the permittivity of the vacuum (8.85×10^{-12} As V^{-1} m^{-1}), ε is the relative permittivity number of the oxide, and d is its thickness. Considering Al_2O_3 and NiO as the main contributors to the passive oxide film, and approximating the value of ε_{Ox} for the sample between $\varepsilon = 10$ for Al_2O_3,[15] and $\varepsilon = 12$ for NiO,[16] the thickness of the formed oxide layer was approximated for each treatment (Table I). The thickness of the oxide film

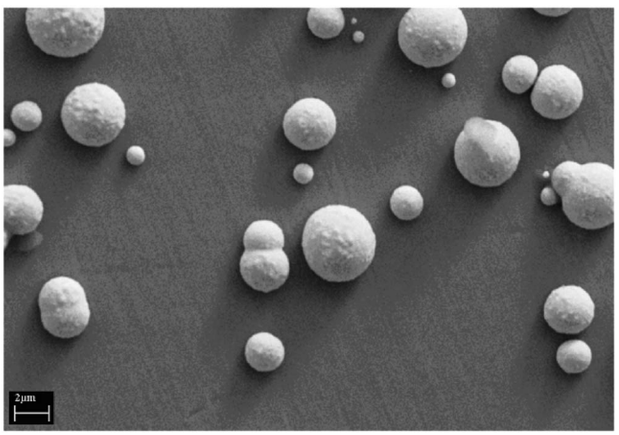

Figure 4. Gold deposited on a NiAl–Re sample after polarization at 0 V.

present in the sample before the anodization process was also calculated from the impedance diagrams recorded prior to the experiments. It was observed that the oxide thickness was larger for the ds-NiAl–Re (67 nm) than for the NiAl system (55 nm), in agreement with the *Z* diagrams depicted in Fig. 3. For both systems the layer increased from an initial value of ~30 nm, thus demonstrating the effect of polarization on growth of the oxide film.

For analysis of pure Re, the total impedance and phase angle were better represented by an equivalent circuit in which the capacitance in parallel to the resistance of the double layer is substituted by a constant phase element (CPE).

After passivation of the samples, gold was electrodeposited by alternating the applied current from cathodic to anodic values. Gold deposits were formed on both the NiAl matrix and the Re fibers in a significant proportion (Fig. 4). The partial activity displayed by the matrix after polarization at 0 V may be the result of the thin Al_2O_3/NiO layer formed at that potential, which would enable the tunnelling of electrons from the inner conductive layers of the matrix to the oxide electrolyte interface. It has been previously suggested that electro-oxidation of NiAl alloys produces oxide layers composed of islands rather than uniform films.[16] The presence of islands, instead of a complete coverage of the surface, would account for the reminiscent electrochemical activity of the matrix. Also, the presence of a large number of imperfections on oxides formed under such a low anodic potential can compromise the stability of the passive oxide, thus favoring its dissolution or partial damaging during the electrodeposition process. This would result in active islands that would serve as nucleation sites.[17] For a binary alloy two effects must be discussed; the first one is the dealloying, and the second is a composition gradient within the oxide normal to the surface. Metals of different nobility have different oxidation tendencies, resulting in a higher concentration of the less noble metal at

Table I. Values of resistance *R*, capacitance *C*, and oxide thickness *d* calculated for NiAl, NiAl–Re, and Re after polarization at different potentials.

	R (MΩ cm^2)	*C* (μF cm^2)	d_{ox} (nm)	CPE-T	CPE-P
NiAl (no treatment)	0.073	21.79	31.7		
ds-NiAl–Re (no treatment)	0.097	24	36.9		
NiAl at 0 V	0.071	16.1	55		
NiAl at 0.7 V	0.71	14.8	60		
ds-NiAl–Re at 0 V	0.35	13.1	67.5		
ds-NiAl–Re at 0.7 V	1.53	9.1	97.4		
Re (no treatment)	15.2			19.6	0.92
Re at 0 V	10.6			19.5	0.92
Re at 0.7 V	14.1			40.8	0.94

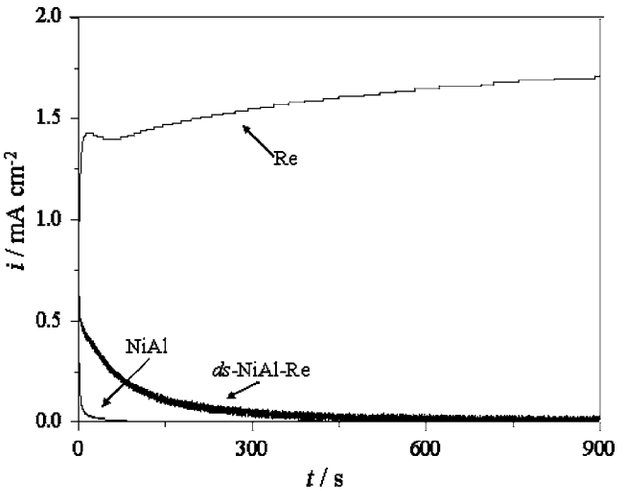

Figure 5. Current transients recorded after polarization of NiAl, NiAl–Re, and Re samples at 0.7 V in acetate buffer pH 6.0.

the electrolyte interface.[18] NiAl would therefore form an outer aluminum oxide film. However, for thin oxide films the gradient drops over a short range and the formation of a protective pure aluminum oxide is not possible. A highly nickel doped oxide with sufficient conductivity may be formed.

Passivation of ds-NiAl–Re at 0.7 V.— According to the *E*–pH diagram (Fig. 1), a polarization of ds-NiAl–Re at anodic potentials and neutral pH values yields the formation of aluminum and nickel oxides on the surface, while the rhenium dissolves into the solution as Re(VII) species, thus creating nanopores along which the deposition of gold has also proved feasible.[8] The current transient recorded for the polarization of ds-NiAl–Re at 0.7 V showed an initial anodic current of 2 mA cm^{-2} which decreased steadily with time until it reached a more or less constant value of 50 μA cm^{-2}. This value remained unchanged for longer polarization times (Fig. 5). The initial high current may be due to the formation of aluminum and nickel oxides, whereas the later steady state may be associated with dissolution of the sample under a constant oxide thickness. For NiAl under the same experimental conditions, the obtained current showed a similar behavior (Fig. 5), although its value decreased during a much shorter time (less than 50 s). The polarization of Re produced a significantly larger anodic current, which seemed to increase slowly with time (Fig. 5). This high anodic current is attributed to the oxidation of elemental rhenium to Re(VII) species (perrhenate). The impedance spectra obtained for each system after polarizations are shown in Fig. 6. As it was observed for the experiments run at 0 V, the evolution of *Z* and phase angle for NiAl and ds-NiAl–Re can be described by a simple equivalent circuit containing the resistance of the electrolyte and the capacitance and resistance of the oxide. From the values of *C* obtained after fitting of the experimental data, the thickness of the oxide layer was calculated according to Eq. 1. In Table I the values of *C* and *R* for each system and the two studied potentials are shown, along with the calculated thickness. The oxide thickness calculated after polarization at 0.7 V is much larger than the initial film present on the sample ($\sim$30 nm). However, the thickness of the oxide layer calculated for the NiAl sample is not much larger than that obtained after polarization at 0 V. These results contrast with those obtained for the ds-NiAl–Re system, which displayed a significant increase in thickness of the oxide film after passivation at 0.7 V (97 nm, compared to 60 nm after 0 V). It is difficult to determine the effect that rhenium oxidation has on the experiments, and further tests should be run in order to obtain an accurate description of the processes involved in the overall reaction and the effect of each one of them on

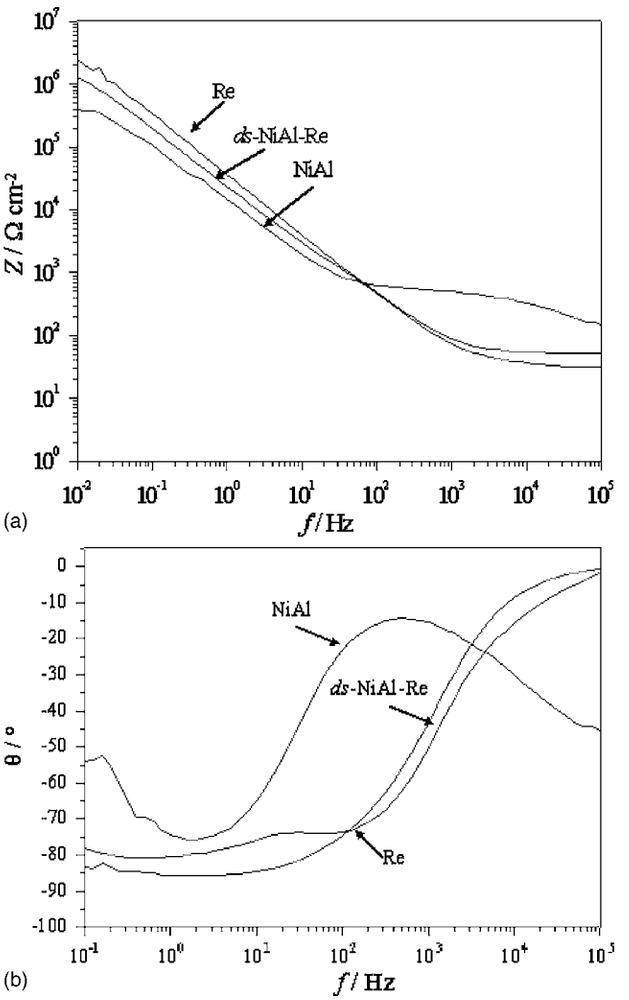

Figure 6. Frequency dependence of *Z* and phase-angle θ for NiAl–Re (light gray line), NiAl (black line), and Re (gray line) after polarization in acetate buffer (pH 6.0) at 0.7 V vs SHE.

the sample treatment. Nevertheless, the results obtained prove that the formation of the oxide layer is strongly dependent on the applied potential, and that an optimal passivation of the studied ds-NiAl–Re samples is only achieved after polarizations at anodic potentials.

The much larger value of $|Z|$ obtained for ds-NiAl–Re samples when compared to NiAl may be the result of an increased resistance due to the presence of pores in the sample. Diffusion of electroactive ions to/from the pores would be slow, contributing to a decrease in the reaction kinetics. For the Re system, the results are fitted more accurately to a circuit containing a CPE, as observed for polarization at 0 V.

The evolution of the oxide film growth at 0.7 V was studied by running short polarizations (30 s) for a ds-NiAl–Re sample, followed by measurements of the total impedance and phase angle after each anodization. The shape of the $|Z|$ and phase diagrams did not change for increasing times, but the total impedance $|Z|$ became larger after longer polarizations (Fig. 7). The results were fitted into the simple equivalent circuit employed in previous experiments, and the values obtained for the inverse capacitance and resistance of the sample after each polarization interval are shown in Fig. 8. The resistance increased quickly during the initial polarization time (0–100 s) from $\sim$4 to $\sim$ 11 MΩ cm^2 and then remained fairly constant for polarization times up to 400 s, after which it decreased again sharply to a value of $\sim$8 MΩ cm^2 for 600 s polarization time.

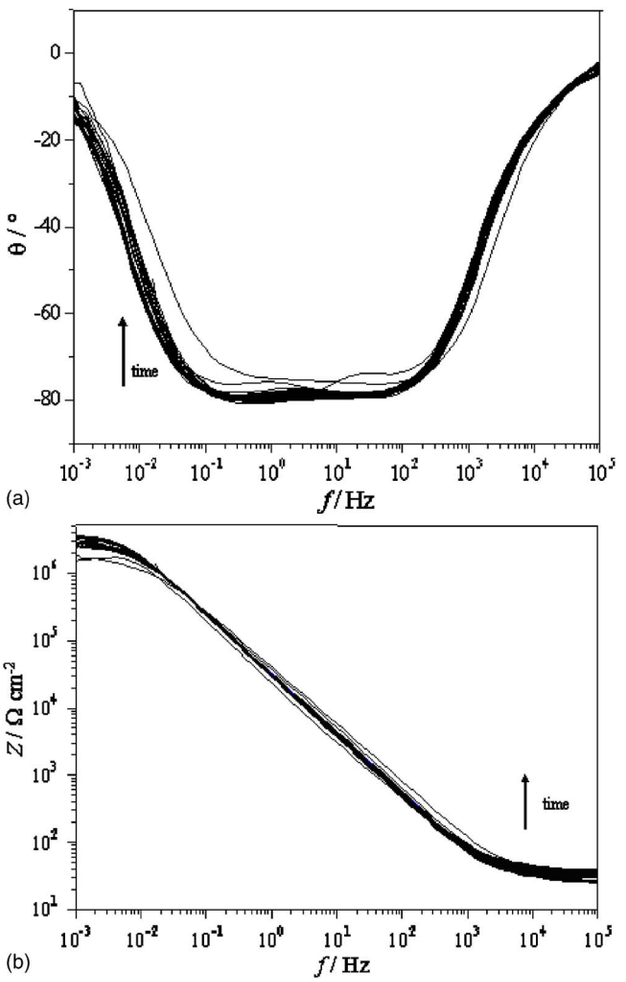

Figure 7. Frequency dependence of Z and phase-angle θ for NiAl–Re after polarization in acetate buffer (pH 6.0) at 0.7 V vs SHE for increasing times.

Longer passivation times displayed a new initial rise of the resistance value to 11 MΩ cm^2, followed by a decrease to the final value of 8 MΩ cm^2. The inverse capacity decreased sharply

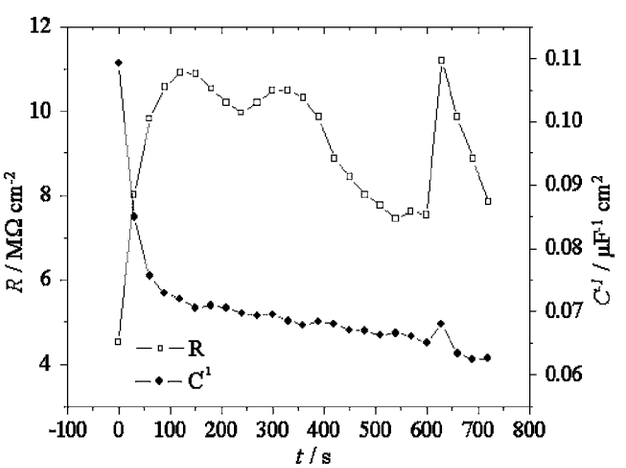

Figure 8. Evolution of resistance and inverse of capacitance for NiAl–Re after longer polarization times at 0.7 V.

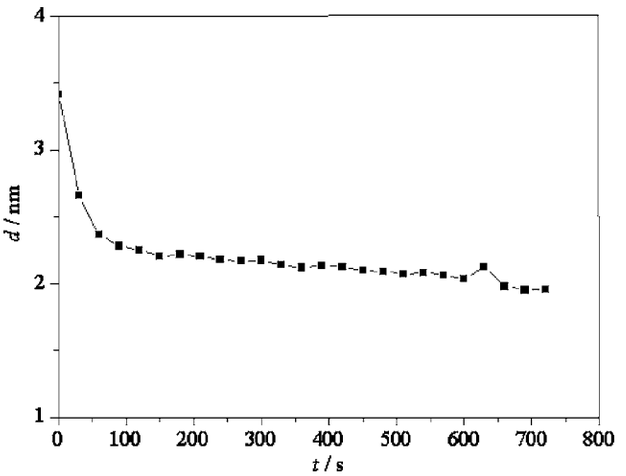

Figure 9. Decrease in thickness of the Al_2O_3 and NiO oxide layer for the NiAl–Re system after longer polarization times at 0.7 V.

during the initial intervals of passivation, from an initial value of 0.11 to 0.07 μF^{-1} cm^2 in 100 s. It remained fairly constant afterward, with a value that fluctuated only slightly in the 0.06–0.07 μF^{-1} cm^2 range. The thickness of the oxide layer after each interval was calculated according to Eq. 1. Contrary to what was expected, the thickness of the oxide film appeared to decrease with each polarization interval (Fig. 9); hence, the calculated thickness decreased abruptly from an initial value of ~90 to 65 nm after only 11 s polarization time. The decrease was then moderate, and after 27 polarization intervals the sample presented a final oxide film with a thickness of 55 nm. The reason for this decrease is not well understood. One reason could be the long time intervals between each two polarization cycles which were determined by the duration of the impedance measurement run after each 30 s passivation cycle. The electrochemical impedance spectroscopy (EIS) analyses were run at open-circuit potential, which has a value of approximately 0.1 V for the ds-NiAl–Re system in neutral acetate buffer. According to the *E*–pH diagram, aluminum forms an oxide at that potential, whereas nickel can be present as an ionic species, thus decreasing the thickness of the total oxide film. Re can also form an oxide at that potential range, which would presumably account for a slight increase in film thickness. The application of such short passivation times (30 s) may also result in the growth of less-stable or more-porous forms of aluminum oxide, which would be more susceptible to corrosion. The oxidation of NiAl can also result in the formation of various spinels, such as $NiAl_2O_4$.[19] This sort of structure would act as a flaw or defect in the oxide film from which corrosion can propagate. The formation of a porous oxide film rather than a compact film may also account for the observed instability.[20] The created pores may also act initially as voids or imperfections in the oxide structure, thus increasing their corrosion rate.

Kinetic studies on the oxidation of NiAl, Re, and ds-NiAl–Re.— The interpretation of the impedance data for the NiAl and ds-NiAl–Re systems obtained in the previous sections was complicated due to the presence of various concomitant processes (NiAl oxidation, Re oxidation/dissolution, and oxide corrosion). In order to determine the effect of each process on the overall reaction, kinetic investigations were run by polarizing NiAl, Re, and ds-NiAl–Re samples at 0.7 V for 24 h. The current transients recorded for each specimen are shown in Fig. 10, where the different regions identified in each graph have also been drawn. For the NiAl system (black graph), two major regions can be identified; the first one can be attributed to the formation and growth of oxides on the surface of

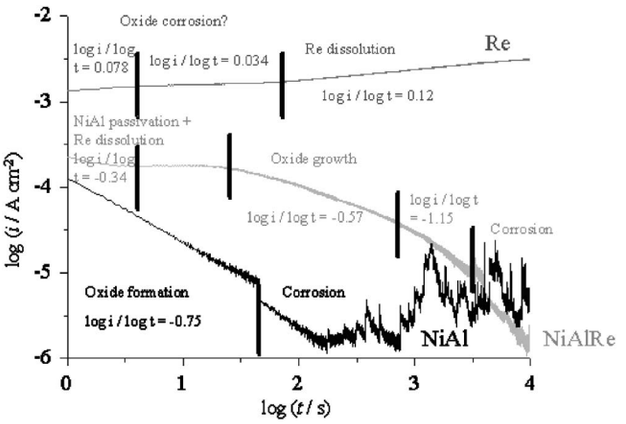

Figure 10. Current transients recorded for the polarization of NiAl (black graph), ds-NiAl–Re (light gray graph), and Re (gray graph) at 0.7 V vs SHE for 20 h.

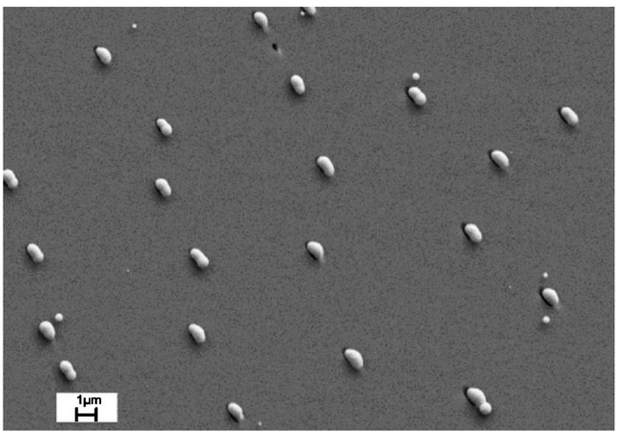

Figure 11. Au deposits observed on a ds-NiAl–Re sample after pretreatment at 0.7 V.

the sample. The oxide is expected to grow according to the high field model. However, the value obtained for the slope is slightly lower than −1.

The current transients obtained for the polarization of ds-NiAl–Re (light gray plot) displayed a more complex appearance, with five different zones distinguished. The first one shows a slight decrease in current density with time, probably due to the initiation of oxide formation. The current density then presents a constant value in the section attributed to the film growth. The fact that the current is not altered suggests that oxide growth is controlled by the diffusion of ions at this stage, most likely from the Al(III) and Ni(II) from the bulk of the alloy, because the surface is expected to be completely covered by an oxide layer at this stage. The following zone shows again a decrease in the current density with time, although such a decrease is much steeper than that observed for the initial measured interval (slope = −0.57). The current density continues to lower its value, until corrosion dominates after ~4 h. The different change observed for the current density in each interval may be due to the formation of different types of oxides. The composition of the oxides may change with time, and longer polarization times could favor the transformation of the initial oxides into a more Ni-rich oxide after the initial enrichment of nickel underneath the oxide resulting from the lower reactivity of nickel. Also, NiO may initially form a hydroxide, which would then dehydrate to create NiO.[16,17] These transformations would result in variations in the current reading according to their kinetics. Additionally, the effect of rhenium oxidation on the process cannot be underestimated. The oxidation of Re(0) to Re(VII) takes place in various steps, which involve the initial formation of ReO_2 or Re_2O_3 oxides, followed by their conversion to ReO_3 and finally ReO_4^-.[13] This stepwise oxidation is better illustrated in the transient recorded for the oxidation of Re (gray plot). Three regions are distinguished in this plot, the first two presenting a small increase in the current density. They can be attributed to the initial oxidation of Re to form the mentioned oxides. The last region is characterized by a large increase in the current value, which is most likely due to oxidation of the Re oxides to perrhenate. In principle, the electrochemical behavior of the ds-NiAl–Re should not depend on the processing parameters of the material, because the eutectic composition, and therefore the volume ratio and the surface ration between minor phase and matrix, are constant.[21,22] However, the kinetic investigation with current transients might show deviations if different time constants can be separated in the time domain due to the overlapping diffusion hemispheres on the adjacent nanowires.

Electrodeposition of gold on ds-NiAl–Re samples after passivation at 0.7 V.— The electrodeposition of gold on the samples passivated at 0.7 V yielded deposits exclusively in the nanopores formed by dissolution of the Re phase (Fig. 11). Only after long electrodeposition times did gold nuclei form on the matrix, probably due to a partial breakage of the oxide layer after such a long exposure. Polarization at a more anodic potential favors the formation of a more perfect and stable oxide, which blocks any electrochemical reaction in the underlying substrate. Therefore, the reduction of Au(I) ions takes place exclusively in the pores, which either remain electrochemically active or are covered by a more fragile oxide layer that prevents the electrons from tunnelling to the metallic substrate or even the ReO_3 oxide with its metallic conductivity.

Conclusions

The polarization pretreatment applied to ds-NiAl–Re eutectics prior to electrodeposition of gold has a strong effect on the plating process. If the passivation is run at low potentials (0 V), the created oxide layer still enables the transfer of electrons from the bulk metal. As a result, the whole sample remains electrochemically active, and gold nuclei are formed all over the surface. Only when the pretreatment is done at high anodic potentials (0.7 V) does the NiAl matrix form a passive oxide layer with an adequate thickness to avoid the electrons tunnelling to the inner conductive sections. As a result, electrodeposition of gold exclusively onto the fibers requires a sample pretreatment at anodic potentials.

The exact determination of the thickness by means of EIS for either low or high anodic polarization does not yield conclusive values of the thickness of the passive film. This might be a result of the formation of a complex mixed nickel–aluminum–oxide with an entirely different permittivity or a parallel connection of reaction impedance on the electroactive minor phase.

Acknowledgments

The financial support of the Deutsche-Forschungs-Gemeinschaft through the project Production of Nanowire Arrays through Directional Solidification and their Application within the DFG Priority Program 1165 Nanowires and Nanotubes from Controlled Synthesis to Function is gratefully acknowledged. The authors are also grateful to Dr. Srdjan Milenkovic for solidification of the employed eutectics.

Max-Planck-Institut für Eisenforschung assisted in meeting the publication costs of this article.

References

1. W. Schwarzacher, O. I. Kasyutich, P. R. Evans, M. G. Darbyshire, G. Zi, V. M. Fedosyuk, F. Rousseaux, E. Cambril, and D. Decanini, *J. Magn. Magn. Mater.*,

198–199, 185 (1999).
2. D. Lincot, *Thin Solid Films*, **487**, 40 (2005).
3. W. Schwarzacher, K. Attenborough, A. Michel, G. Nabiyouni, and J. P. Meier, *J. Magn. Magn. Mater.*, **165**, 23 (1997).
4. K. Kim, M. Kim, and S. M. Cho, *Mater. Chem. Phys.*, **96**, 278 (2006).
5. H. Masuda and K. Fukuda, *Science*, **268**, 1466 (1995).
6. K. R. Pirota, D. Navas, M. Hernandez-Velez, K. Nielsch, and M. Vazquez, *J. Alloys Compd.*, **369**, 18 (2004).
7. A. Aguilera, V. Jayaraman, S. Sanagapalli, R. S. Singh, V. Jayaraman, K. Sampson, and V. P. Singh, *Sol. Energy Mater. Sol. Cells*, **90**, 713 (2006).
8. A. Saedi and M. Ghorbani, *Mater. Chem. Phys.*, **91**, 417 (2005).
9. A. Mozalev, A. Poznyak, I. Mozaleva, and A. W. Hassel, *Electrochem. Commun.*, **3**, 299 (2001).
10. B. Bello Rodriguez and A. W. Hassel, *J. Electrochem. Soc.*, **153**, C33 (2006).
11. A. W. Hassel, B. Bello Rodriguez, S. Milenkovic, and A. Schneider, *Electrochim. Acta*, **50**, 3033 (2005).
12. D. Dobrev, J. Vetter, N. Angert, and R. Neumann, *Electrochim. Acta*, **45**, 3117 (2000).
13. M. Pourbaix, *Atlas of Electrochemical Equilibria in Aqueos Solutions*, National Association of Corrosion Engineers, Houston, TX (1974).
14. B. MacDougall and M. Cohen, *J. Electrochem. Soc.*, **121**, 1152 (1974).
15. D. W. Letcher, T. J. Cardwell, and R. J. Magee, *J. Electroanal. Chem.*, **25**, 472 (1970).
16. S. Gudić, J. Radošević, and M. Kliškić, *Electrochim. Acta*, **47**, 3009 (2002).
17. *Gmelins Handbuch der Anorganischen Chemie*, Verlag Chemie GmbH, Weinheim (1966).
18. S. Brittman, A. J. Smith, S. Milenkovic, and A. W. Hassel, *Electrochim. Acta*, **53**, 324 (2007).
19. M. S. Zei, C. S. Lin, W. H. Wen, C. I. Chiang, and M. F. Luo, *Surf. Sci.*, **600**, 1942 (2006).
20. B. MacDougall, *J. Electrochem. Soc.*, **127**, 789 (1980).
21. S. Milenkovic, A. W. Hassel, and A. Schneider, *Nano Lett.*, **6**, 794 (2006).
22. S. Milenkovic, A. Schneider, and A. W. Hassel, *Gold Bull.*, **39**, 185 (2006).